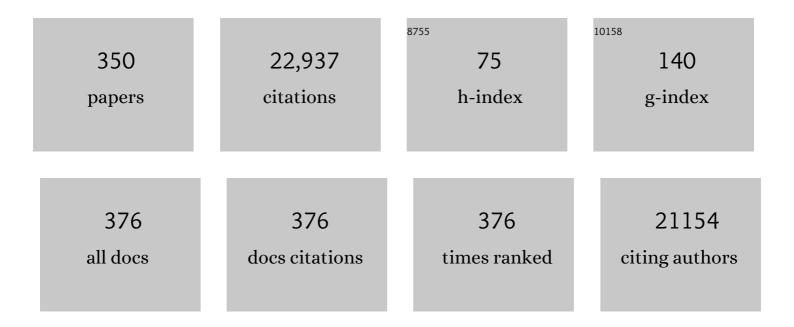
List of Publications by Year in descending order

Source: https://exaly.com/author-pdf/1675695/publications.pdf Version: 2024-02-01



| # | Article | IF | CITATIONS |
|----|---|------|-----------|
| 1 | A Computational Monte Carlo Simulation Strategy to Determine the Temporal Ordering of Abnormal Age Onset Among Biomarkers of Alzheimer's Disease. IEEE/ACM Transactions on Computational Biology and Bioinformatics, 2022, 19, 2613-2622. | 3.0 | 4 |
| 2 | Limitations of clinical trial sample size estimate by subtraction of two measurements. Statistics in Medicine, 2022, 41, 1137-1147. | 1.6 | 2 |
| 3 | Brain structural and functional anomalies associated with simultanagnosia in patients with posterior cortical atrophy. Brain Imaging and Behavior, 2022, 16, 1148-1162. | 2.1 | 9 |
| 4 | Studying APOE É›4 Allele Dose Effects withÂa Univariate Morphometry Biomarker. Journal of Alzheimer's Disease, 2022, 85, 1233-1250. | 2.6 | 1 |
| 5 | Sex differences in cognitive resilience in preclinical autosomalâ€dominant Alzheimer's disease carriers and nonâ€carriers: Baseline findings from the API ADAD Colombia Trial. Alzheimer's and Dementia, 2022, 18, 2272-2282. | 0.8 | 10 |
| 6 | Deep residual inception encoderâ€decoder network for amyloid PET harmonization. Alzheimer's and Dementia, 2022, 18, 2448-2457. | 0.8 | 10 |
| 7 | Hemispheric Asymmetry and Atypical Lobar Progression of Alzheimer-Type Tauopathy. Journal of Neuropathology and Experimental Neurology, 2022, 81, 158-171. | 1.7 | 2 |
| 8 | Reconfigured metabolism brain network in asymptomatic microtubule-associated protein tau mutation carriers: a graph theoretical analysis. Alzheimer's Research and Therapy, 2022, 14, 52. | 6.2 | 6 |
| 9 | Investigating the Effect of Tau Deposition and Apoe on Hippocampal Morphometry in Alzheimer's Disease: A Federated Chow Test Model. , 2022, , . | | 1 |
| 10 | Glucose metabolism patterns: A potential index to characterize brain ageing and predict high conversion risk into cognitive impairment. GeroScience, 2022, 44, 2319-2336. | 4.6 | 8 |
| 11 | White matter hyperintensities are a prominent feature of autosomalÂdominant Alzheimer's disease that emerge prior to dementia. Alzheimer's Research and Therapy, 2022, 14, . | 6.2 | 12 |
| 12 | A novel transfer learning model for predictive analytics using incomplete multimodality data. IISE Transactions, 2021, 53, 1010-1022. | 2.4 | 5 |
| 13 | Developing univariate neurodegeneration biomarkers with low-rank and sparse subspace decomposition. Medical Image Analysis, 2021, 67, 101877. | 11.6 | 10 |
| 14 | Relationship between the disrupted topological efficiency of the structural brain connectome and glucose hypometabolism in normal aging. NeuroImage, 2021, 226, 117591. | 4.2 | 15 |
| 15 | PET evidence of preclinical cerebellar amyloid plaque deposition in autosomal dominant Alzheimer's disease-causing Presenilin-1 E280A mutation carriers. NeuroImage: Clinical, 2021, 31, 102749. | 2.7 | 8 |
| 16 | Cortical thickness across the lifespan in a Colombian cohort with autosomalâ€dominant Alzheimer's disease: A crossâ€sectional study. Alzheimer's and Dementia: Diagnosis, Assessment and Disease Monitoring, 2021, 13, e12233. | 2.4 | 2 |
| 17 | A 36-week multicenter, randomized, double-blind, placebo-controlled, parallel-group, phase 3 clinical trial of sodium oligomannate for mild-to-moderate Alzheimer's dementia. Alzheimer's Research and Therapy, 2021, 13, 62. | 6.2 | 99 |
| 18 | Early prevention of cognitive impairment in the community population: The Beijing Aging Brain Rejuvenation Initiative. Alzheimer's and Dementia, 2021, 17, 1610-1618. | 0.8 | 28 |

| # | Article | IF | CITATIONS |
|----|---|------|-----------|
| 19 | Improved Prediction of Imminent Progression to Clinically Significant Memory Decline Using Surface Multivariate Morphometry Statistics and Sparse Coding. Journal of Alzheimer's Disease, 2021, 81, 209-220. | 2.6 | 6 |
| 20 | Predicting future cognitive decline with hyperbolic stochastic coding. Medical Image Analysis, 2021, 70, 102009. | 11.6 | 2 |
| 21 | Plasma Apolipoprotein E3 and Glucose Levels Are Associated in APOE É>3/É>4 Carriers. Journal of Alzheimer's Disease, 2021, 81, 339-354. | 2.6 | 13 |
| 22 | Disrupted anterior and posterior hippocampal structural networks correlate impaired verbal memory and spatial memory in different subtypes of mild cognitive impairment. European Journal of Neurology, 2021, 28, 3955-3964. | 3.3 | 5 |
| 23 | Community-based Model for Dementia Risk Screening: The Beijing Aging Brain Rejuvenation Initiative (BABRI) Brain Health System. Journal of the American Medical Directors Association, 2021, 22, 1500-1506.e3. | 2.5 | 7 |
| 24 | Predicting Brain Amyloid Using Multivariate Morphometry Statistics, Sparse Coding, and Correntropy: Validation in 1,101 Individuals From the ADNI and OASIS Databases. Frontiers in Neuroscience, 2021, 15, 669595. | 2.8 | 15 |
| 25 | Accelerated Brain Aging in Amnestic Mild Cognitive Impairment: Relationships with Individual Cognitive Decline, Risk Factors for Alzheimer Disease, and Clinical Progression. Radiology: Artificial Intelligence, 2021, 3, e200171. | 5.8 | 8 |
| 26 | Accelerated functional brain aging in pre-clinical familial Alzheimer's disease. Nature Communications, 2021, 12, 5346. | 12.8 | 43 |
| 27 | Positron emission tomography imaging of serotonin degeneration and beta-amyloid deposition in late-life depression evaluated with multi-modal partial least squares. Translational Psychiatry, 2021, 11, 473. | 4.8 | 18 |
| 28 | Federated Morphometry Feature Selection for Hippocampal Morphometry Associated Beta-Amyloid and Tau Pathology. Frontiers in Neuroscience, 2021, 15, 762458. | 2.8 | 5 |
| 29 | Improved comparability between measurements of mean cortical amyloid plaque burden derived from different PET tracers using multiple regionsâ€ofâ€interest and machine learning. Alzheimer's and Dementia, 2021, 17, . | 0.8 | 0 |
| 30 | Predicting Tau accumulation in cerebral cortex with multivariate MRI morphometry measurements, sparse coding, and correntropy. , 2021, 12088, . | | 1 |
| 31 | Brain imaging measurements of fibrillar amyloidâ€Î² burden, paired helical filament tau burden, and atrophy in cognitively unimpaired persons with two, one, and no copies of the <i>APOE ε4</i> allele. Alzheimer's and Dementia, 2020, 16, 598-609. | 0.8 | 23 |
| 32 | Age-Related Regional Network Covariance of Magnetic Resonance Imaging Gray Matter in the Rat. Frontiers in Aging Neuroscience, 2020, 12, 267. | 3.4 | 18 |
| 33 | Longitudinal white matter and cognitive development in pediatric carriers of the apolipoprotein ε4 allele. NeuroImage, 2020, 222, 117243. | 4.2 | 14 |
| 34 | Higher CSF sTREM2 attenuates ApoE4-related risk for cognitive decline and neurodegeneration. Molecular Neurodegeneration, 2020, 15, 57. | 10.8 | 33 |
| 35 | Interaction Between BDNF Val66Met and APOE4 on Biomarkers of Alzheimer's Disease and Cognitive Decline. Journal of Alzheimer's Disease, 2020, 78, 721-734. | 2.6 | 11 |
| 36 | Applying surface-based morphometry to study ventricular abnormalities of cognitively unimpaired subjects prior to clinically significant memory decline. NeuroImage: Clinical, 2020, 27, 102338. | 2.7 | 18 |

| # | Article | IF | CITATIONS |
|----|---|------|-----------|
| 37 | Noninvasive Input Function Acquisition and Simultaneous Estimations With Physiological Parameters for PET Quantification: A Brief Review. IEEE Transactions on Radiation and Plasma Medical Sciences, 2020, 4, 676-683. | 3.7 | 10 |
| 38 | Baseline demographic, clinical, and cognitive characteristics of the Alzheimer's Prevention Initiative (API) Autosomalâ€Dominant Alzheimer's Disease Colombia Trial. Alzheimer's and Dementia, 2020, 16, 1023-1030. | 0.8 | 15 |
| 39 | Braak Stage, Cerebral Amyloid Angiopathy, and Cognitive Decline in Early Alzheimer's Disease. Journal of Alzheimer's Disease, 2020, 74, 189-197. | 2.6 | 18 |
| 40 | Computing Univariate Neurodegenerative Biomarkers with Volumetric Optimal Transportation: A Pilot Study. Neuroinformatics, 2020, 18, 531-548. | 2.8 | 3 |
| 41 | Age-Related Decline in the Topological Efficiency of the Brain Structural Connectome and Cognitive Aging. Cerebral Cortex, 2020, 30, 4651-4661. | 2.9 | 22 |
| 42 | APOE Îμ4 allele accelerates age-related multi-cognitive decline and white matter damage in non-demented elderly. Aging, 2020, 12, 12019-12031. | 3.1 | 5 |
| 43 | Female-specific effects of the catechol-O-methyl transferase Val158Met gene polymorphism on working memory-related brain function. Aging, 2020, 12, 23900-23916. | 3.1 | 0 |
| 44 | Visualizing Alzheimer's disease progression in low dimensional manifolds. Heliyon, 2019, 5, e02216. | 3.2 | 6 |
| 45 | Effect of AZD0530 on Cerebral Metabolic Decline in Alzheimer Disease. JAMA Neurology, 2019, 76, 1219. | 9.0 | 107 |
| 46 | Changes in the Functional and Structural Default Mode Network Across the Adult Lifespan Based on Partial Least Squares. IEEE Access, 2019, 7, 82256-82265. | 4.2 | 6 |
| 47 | White Matter Microstructural Change Contributes to Worse Cognitive Function in Patients With Type 2 Diabetes. Diabetes, 2019, 68, 2085-2094. | 0.6 | 26 |
| 48 | Applying surface-based hippocampal morphometry to study APOE-E4 allele dose effects in cognitively unimpaired subjects. NeuroImage: Clinical, 2019, 22, 101744. | 2.7 | 40 |
| 49 | Tau Positron-Emission Tomography in Former National Football League Players. New England Journal of Medicine, 2019, 380, 1716-1725. | 27.0 | 165 |
| 50 | Striatal amyloid is associated with tauopathy and memory decline in familial Alzheimer's disease. Alzheimer's Research and Therapy, 2019, 11, 17. | 6.2 | 26 |
| 51 | Cerebral Amyloid Angiopathy and Neuritic Plaque Pathology Correlate with Cognitive Decline in Elderly Non-Demented Individuals. Journal of Alzheimer's Disease, 2019, 67, 411-422. | 2.6 | 8 |
| 52 | A concise and persistent feature to study brain restingâ€state network dynamics: Findings from the Alzheimer's Disease Neuroimaging Initiative. Human Brain Mapping, 2019, 40, 1062-1081. | 3.6 | 26 |
| 53 | The positive impacts of early-life education on cognition, leisure activity, and brain structure in healthy aging. Aging, 2019, 11, 4923-4942. | 3.1 | 54 |
| 54 | Aberrant Connectivity in Mild Cognitive Impairment and Alzheimer Disease Revealed by Multimodal Neuroimaging Data. Neurodegenerative Diseases, 2018, 18, 5-18. | 1.4 | 11 |

| # | Article | IF | CITATIONS |
|----|---|-----|-----------|
| 55 | Association Between Amyloid and Tau Accumulation in Young Adults With Autosomal Dominant Alzheimer Disease. JAMA Neurology, 2018, 75, 548. | 9.0 | 137 |
| 56 | <i>APOE</i> influences working memory in nonâ€demented elderly through an interaction with <i>SPON1</i> rs2618516. Human Brain Mapping, 2018, 39, 2859-2867. | 3.6 | 11 |
| 57 | Prevalence of the apolipoprotein E ε4 allele in amyloid β positive subjects across the spectrum of Alzheimer's disease. Alzheimer's and Dementia, 2018, 14, 913-924. | 0.8 | 58 |
| 58 | Longitudinal Changes in Serum Glucose Levels are Associated with Metabolic Changes in Alzheimer's Disease Related Brain Regions. Journal of Alzheimer's Disease, 2018, 62, 833-840. | 2.6 | 7 |
| 59 | The Alzheimer's Prevention Initiative Autosomala&Dominant Alzheimer's Disease Trial: A study of crenezumab versus placebo in preclinical <i>PSEN1</i> E280A mutation carriers to evaluate efficacy and safety in the treatment of autosomala&dominant Alzheimer's disease, including a placeboâ&treated noncarrier cohort. Alzheimer's and Dementia: Translational Research and Clinical Interventions, 2018, | 3.7 | 107 |
| 60 | The Interactive Effects of Age and PICALM rs541458 Polymorphism on Cognitive Performance, Brain Structure, and Function in Non-demented Elderly. Molecular Neurobiology, 2018, 55, 1271-1283. | 4.0 | 10 |
| 61 | P1â€454: RELATIONSHIPS BETWEEN MEAN CORTICAL AMYLOID BURDEN AND REGIONAL GRAY MATTER REDUCTIONS IN ALZHEIMER'S DEMENTIA, MILD COGNITIVE IMPAIRMENT AND UNIMPAIRED OLDER ADULTS. Alzheimer's and Dementia, 2018, 14, P490. | 0.8 | 0 |
| 62 | ICâ€₽â€003: RELATIONSHIPS BETWEEN MEAN CORTICAL AMYLOID BURDEN AND REGIONAL GRAY MATTER REDUCTIONS IN ALZHEIMER'S DEMENTIA, MILD COGNITIVE IMPAIRMENT AND UNIMPAIRED OLDER ADULTS. Alzheimer's and Dementia, 2018, 14, P15. | 0.8 | 0 |
| 63 | Amyloid positron emission tomography and cerebrospinal fluid results from a crenezumab anti-amyloid-beta antibody double-blind, placebo-controlled, randomized phase II study in mild-to-moderate Alzheimer's disease (BLAZE). Alzheimer's Research and Therapy, 2018, 10, 96. | 6.2 | 109 |
| 64 | Hippocampus morphometry study on pathology-confirmed Alzheimer's disease patients with surface multivariate morphometry statistics. , 2018, 2018, 1555-1559. | | 17 |
| 65 | Cognitive composite score association with Alzheimer's disease plaque and tangle pathology. Alzheimer's Research and Therapy, 2018, 10, 90. | 6.2 | 23 |
| 66 | Predicting Imminent Progression to Clinically Significant Memory Decline Using Volumetric MRI and FDG PET. Journal of Alzheimer's Disease, 2018, 63, 603-615. | 2.6 | 12 |
| 67 | Left lateralized cerebral glucose metabolism declines in amyloid-β positive persons with mild cognitive impairment. NeuroImage: Clinical, 2018, 20, 286-296. | 2.7 | 64 |
| 68 | Combinations of Multiple Neuroimaging Markers using Logistic Regression for Auxiliary Diagnosis of Alzheimer Disease and Mild Cognitive Impairment. Neurodegenerative Diseases, 2018, 18, 91-106. | 1.4 | 3 |
| 69 | Beijing Aging Brain Rejuvenation Initiative: aging with grace. Scientia Sinica Vitae, 2018, 48, 721-734. | 0.3 | 10 |
| 70 | ADMultiImg: a novel missing modality transfer learning based CAD system for diagnosis of MCI due to AD using incomplete multi-modality imaging data. , 2018, , . | | 0 |
| 71 | Peripheral apoE isoform levels in cognitively normal APOE ε3/ε4 individuals are associated with regional gray matter volume and cerebral glucose metabolism. Alzheimer's Research and Therapy, 2017, 9, 5. | 6.2 | 29 |
| 72 | Design of a short nonuniform acquisition protocol for quantitative analysis in dynamic cardiac SPECT imaging - a retrospective ¹²³ I-MIBG animal study. Medical Physics, 2017, 44, 3639-3649. | 3.0 | 1 |

| # | Article | IF | CITATIONS |
|----|---|------------|-----------|
| 73 | Multi-feature kernel discriminant dictionary learning for face recognition. Pattern Recognition, 2017, 66, 404-411. | 8.1 | 40 |
| 74 | Added value and limitations of amyloid-PET imaging: review and analysis of selected cases of mild cognitive impairment and dementia. Neurocase, 2017, 23, 41-51. | 0.6 | 10 |
| 75 | Statistical considerations for assessing cognition and neuropathology associations in preclinical Alzheimer's disease. Biostatistics and Epidemiology, 2017, 1, 92-104. | 0.4 | 4 |
| 76 | Subjective memory complaints in preclinical autosomal dominant Alzheimer disease. Neurology, 2017, 89, 1464-1470. | 1.1 | 23 |
| 77 | Multi-modal discriminative dictionary learning for Alzheimer's disease and mild cognitive impairment. Computer Methods and Programs in Biomedicine, 2017, 150, 1-8. | 4.7 | 30 |
| 78 | [P4–247]: LEFT LATERALIZED CEREBRAL GLUCOSE METABOLISM DECLINES IN AMYLOIDâ€Î²â€POSITIVE SUBJE WITH MILD COGNITIVE IMPAIRMENT. Alzheimer's and Dementia, 2017, 13, P1372. | CTS 0.8 | 0 |
| 79 | [ICâ€₽â€210]: LEFT LATERALIZED CEREBRAL GLUCOSE METABOLISM DECLINES IN AMYLOIDâ€Î²â€" POSITIVE SU WITH MILD COGNITIVE IMPAIRMENT. Alzheimer's and Dementia, 2017, 13, P152. | BIECTS | 0 |
| 80 | Impact statement: Sequential biomarker testing for Alzheimer's disease early diagnosis. IISE Transactions on Healthcare Systems Engineering, 2017, 7, 247-247. | 1.7 | 0 |
| 81 | An 8-week open label trial of l-Threonic Acid Magnesium Salt in patients with mild to moderate dementia. Personalized Medicine in Psychiatry, 2017, 4-6, 7-12. | 0.1 | 4 |
| 82 | Disrupted Brain Structural Connectivity: Pathological Interactions Between Genetic APOE ε4 Status and Developed MCI Condition. Molecular Neurobiology, 2017, 54, 6999-7007. | 4.0 | 18 |
| 83 | <i><scp>SORL</scp>1</i> rs1699102 polymorphism modulates ageâ€related cognitive decline and gray matter volume reduction in nonâ€demented individuals. European Journal of Neurology, 2017, 24, 187-194. | 3.3 | 11 |
| 84 | Precuneus degeneration in nondemented elderly individuals with <i>APOE</i> ɛ4: Evidence from structural and functional MRI analyses. Human Brain Mapping, 2017, 38, 271-282. | 3.6 | 18 |
| 85 | Inflection Point in Course of Mild Cognitive Impairment: Increased Functional Connectivity of Default Mode Network. Journal of Alzheimer's Disease, 2017, 60, 679-690. | 2.6 | 15 |
| 86 | [P3–032]: SSRI USE ASSOCIATED WITH REDUCED AMYLOID BURDEN IN PERSONS WITH COMBATâ€RELATED PTSD: PRELIMINARY FINDINGS FROM ADNIâ€ĐOD. Alzheimer's and Dementia, 2017, 13, P942. | 0.8 | 0 |
| 87 | [ICâ€Pâ€209]: CAVEATS WHEN SUBTRACTING TWO SERIAL MEASUREMENTS TO ESTIMATE THE NUMBER OF PARTICIPANTS NEEDED FOR CLINICAL TRIALS THAT ARE LONGER OR SHORTER THAN THE OBSERVED MEASUREMENT INTERVAL. Alzheimer's and Dementia, 2017, 13, P151. | 0.8 | 0 |
| 88 | [ICâ€₽â€211]: A COMPUTATIONAL MONTE CARLO SIMULATION STRATEGY TO COMPARE THE ONSET OF DIFFER BIOMARKER AND COGNITIVE CHANGES. Alzheimer's and Dementia, 2017, 13, P152. | ENT 0.8 | 0 |
| 89 | [P1–260]: A COMPUTATIONAL MONTEâ€CARLO SIMULATION STRATEGY TO COMPARE THE ONSET OF DIFFERE BIOMARKER AND COGNITIVE CHANGES. Alzheimer's and Dementia, 2017, 13, P349. | ENT 0.8 | 0 |
| 90 | [P1–261]: TRACKING ALZHEIMER's DISEASE PROGRESSION BY NONâ€LINEAR DIMENSION REDUCTION OF BRA MRI FEATURES. Alzheimer's and Dementia, 2017, 13, P349. | IN 0.8 | 0 |

KEWEI CHEN

| # | Article | IF | CITATIONS |
|-----|---|-----|-----------|
| 91 | [P2–333]: CAVEATS WHEN SUBTRACTING TWO SERIAL MEASUREMENTS TO ESTIMATE THE NUMBER OF PARTICIPANTS NEEDED FOR CLINICAL TRIALS THAT ARE LONGER OR SHORTER THAN THE OBSERVED MEASUREMENT INTERVAL. Alzheimer's and Dementia, 2017, 13, P748. | 0.8 | 0 |
| 92 | Diagnosis on Mild Cognitive Impairment Patients for Alzheimer Disease with Missing Data. , 2017, , . | | 0 |
| 93 | An Optimal Transportation Based Univariate Neuroimaging Index. , 2017, , . | | 1 |
| 94 | Multistage Grading of Amnestic Mild Cognitive Impairment: The Associated Brain Gray Matter Volume and Cognitive Behavior Characterization. Frontiers in Aging Neuroscience, 2017, 8, 332. | 3.4 | 4 |
| 95 | Blood Pressure Control in Aging Predicts Cerebral Atrophy Related to Small-Vessel White Matter Lesions. Frontiers in Aging Neuroscience, 2017, 9, 132. | 3.4 | 24 |
| 96 | Structural Brain Network Changes across the Adult Lifespan. Frontiers in Aging Neuroscience, 2017, 9, 275. | 3.4 | 42 |
| 97 | Prediction of Mild Cognitive Impairment Conversion Using a Combination of Independent Component Analysis and the Cox Model. Frontiers in Human Neuroscience, 2017, 11, 33. | 2.0 | 66 |
| 98 | Static and Dynamic Cognitive Reserve Proxy Measures: Interactions with Alzheimer's Disease Neuropathology and Cognition. , 2017, 07, . | | 13 |
| 99 | Classification of Alzheimer's Disease, Mild Cognitive Impairment, and Cognitively Unimpaired Individuals Using Multi-feature Kernel Discriminant Dictionary Learning. Frontiers in Computational Neuroscience, 2017, 11, 117. | 2.1 | 22 |
| 100 | An Optimal Transportation based Univariate Neuroimaging Index. Proceedings of the IEEE International Conference on Computer Vision, 2017, 2017, 182-191. | 0.0 | 2 |
| 101 | A Triple Network Connectivity Study of Large-Scale Brain Systems in Cognitively Normal APOE4 Carriers. Frontiers in Aging Neuroscience, 2016, 8, 231. | 3.4 | 39 |
| 102 | Quantitative Amyloid Imaging in Autosomal Dominant Alzheimer's Disease: Results from the DIAN Study Group. PLoS ONE, 2016, 11, e0152082. | 2.5 | 45 |
| 103 | Is in vivo amyloid distribution asymmetric in primary progressive aphasia?. Annals of Neurology, 2016, 79, 496-501. | 5.3 | 17 |
| 104 | The Effects of an APOE Promoter Polymorphism on Human White Matter Connectivity during Non-Demented Aging. Journal of Alzheimer's Disease, 2016, 55, 77-87. | 2.6 | 12 |
| 105 | Multimodal Classification of Mild Cognitive Impairment Based on Partial Least Squares. Journal of Alzheimer's Disease, 2016, 54, 359-371. | 2.6 | 39 |
| 106 | Prediction of Progressive Mild Cognitive Impairment by Multi-Modal Neuroimaging Biomarkers. Journal of Alzheimer's Disease, 2016, 51, 1045-1056. | 2.6 | 62 |
| 107 | Morphometric analysis of hippocampus and lateral ventricle reveals regional difference between cognitively stable and declining persons. , 2016, 2016, 14-18. | | 5 |
| 108 | P3â€285: Patchâ€Based Sparse Coding and Multivariate Surface Morphometry for Predicting Amnestic Mild Cognitive Impairment and Alzheimer'S Disease in Cognitively Unimpaired Individuals. Alzheimer's and Dementia, 2016, 12, P947. | 0.8 | 3 |

| # | Article | IF | CITATIONS |
|-----|--|-----|-----------|
| 109 | A Two-Year Treatment of Amnestic Mild Cognitive Impairment using a Compound Chinese Medicine: A Placebo Controlled Randomized Trial. Scientific Reports, 2016, 6, 28982. | 3.3 | 18 |
| 110 | P1-292: Lower Frontal Amyloid Burden in Antidepressant Users: Preliminary Findings From Persons With and Without Post-Traumatic Stress Disorder in The ADNI DOD Study. , 2016, 12, P532-P533. | | 0 |
| 111 | P2â€243: Higher BMI is Associated with Greater Cerebral Glucose Metabolism in Late Middleâ€Aged and Elderly Subjects Regardless of <i>APOE</i> ε4 Genotype. Alzheimer's and Dementia, 2016, 12, P717. | 0.8 | 0 |
| 112 | Supervised within-class-similar discriminative dictionary learning for face recognition. Journal of Visual Communication and Image Representation, 2016, 38, 561-572. | 2.8 | 13 |
| 113 | Cortical sources of resting state EEG rhythms are related to brain hypometabolism in subjects with Alzheimer's disease: an EEG-PET study. Neurobiology of Aging, 2016, 48, 122-134. | 3.1 | 53 |
| 114 | A CAD Tribute to Gerald Farin. CAD Computer Aided Design, 2016, 80, 1-5. | 2.7 | 0 |
| 115 | Applying sparse coding to surface multivariate tensor-based morphometry to predict future cognitive decline. , 2016, 2016, 646-650. | | 25 |
| 116 | Disrupted White Matter Network and Cognitive Decline in Type 2 Diabetes Patients. Journal of Alzheimer's Disease, 2016, 53, 185-195. | 2.6 | 39 |
| 117 | Hyperbolic Space Sparse Coding with Its Application on Prediction of Alzheimer's Disease in Mild Cognitive Impairment. Lecture Notes in Computer Science, 2016, 9900, 326-334. | 1.3 | 17 |
| 118 | Neuritic and Diffuse Plaque Associations with Memory in Non-Cognitively Impaired Elderly. Journal of Alzheimer's Disease, 2016, 53, 1641-1652. | 2.6 | 48 |
| 119 | Gender Differences in Alzheimer Disease: Brain Atrophy, Histopathology Burden, and Cognition. Journal of Neuropathology and Experimental Neurology, 2016, 75, 748-754. | 1.7 | 82 |
| 120 | Disrupted white matter structure underlies cognitive deficit in hypertensive patients. European Radiology, 2016, 26, 2899-2907. | 4.5 | 20 |
| 121 | P3-169: Reduced default network functional connectivity and verbal learning in cognitively unimpaired late middle-aged and older adults: Exploratory findings from the arizona ApoE cohort study. , 2015, 11, P694-P694. | | 0 |
| 122 | Effects of <scp><i>APOE</i></scp> promoter polymorphism on the topological organization of brain structural connectome in nondemented elderly. Human Brain Mapping, 2015, 36, 4847-4858. | 3.6 | 21 |
| 123 | A potential role for the midbrain in integrating fatâ€free mass determined energy needs: An H ₂ ¹⁵ 0 PET study. Human Brain Mapping, 2015, 36, 2406-2415. | 3.6 | 19 |
| 124 | Meet Our Editor:. Neuroscience and Biomedical Engineering, 2015, 3, 1-1. | 0.4 | 0 |
| 125 | Dynamic FDG-PET Imaging to Differentiate Malignancies from Inflammation in Subcutaneous and In Situ Mouse Model for Non-Small Cell Lung Carcinoma (NSCLC). PLoS ONE, 2015, 10, e0139089. | 2.5 | 22 |
| 126 | Longitudinal Evaluation of Sympathetic Nervous System and Perfusion in Normal and Spontaneously Hypertensive Rat Hearts with Dynamic Single-Photon Emission Computed Tomography. Molecular Imaging, 2015, 14, 7290.2015.00012. | 1.4 | 3 |

| # | Article | IF | CITATIONS |
|-----|---|-----|-----------|
| 127 | Improved Power for Characterizing Longitudinal Amyloid-β PET Changes and Evaluating Amyloid-Modifying Treatments with a Cerebral White Matter Reference Region. Journal of Nuclear Medicine, 2015, 56, 560-566. | 5.0 | 122 |
| 128 | Disrupted Functional and Structural Networks in Cognitively Normal Elderly Subjects with the APOE ɛ4 Allele. Neuropsychopharmacology, 2015, 40, 1181-1191. | 5.4 | 60 |
| 129 | Structural covariance networks across healthy young adults and their consistency. Journal of Magnetic Resonance Imaging, 2015, 42, 261-268. | 3.4 | 15 |
| 130 | The Alzheimer's Disease Neuroimaging Initiative 2 PET Core: 2015. Alzheimer's and Dementia, 2015, 11, 757-771. | 0.8 | 199 |
| 131 | Memory, executive, and multidomain subtle cognitive impairment. Neurology, 2015, 85, 144-153. | 1.1 | 42 |
| 132 | Brain Imaging and Blood Biomarker Abnormalities in Children With Autosomal Dominant Alzheimer Disease. JAMA Neurology, 2015, 72, 912. | 9.0 | 94 |
| 133 | Florbetapir PET, FDG PET, and MRI in Down syndrome individuals with and without Alzheimer's dementia. Alzheimer's and Dementia, 2015, 11, 994-1004. | 0.8 | 58 |
| 134 | Sensitivity to change and prediction of global change for the Alzheimer's Questionnaire. Alzheimer's Research and Therapy, 2015, 7, 1. | 6.2 | 67 |
| 135 | A phase Ib multiple ascending dose study of the safety, tolerability, and central nervous system availability of AZD0530 (saracatinib) in Alzheimer's disease. Alzheimer's Research and Therapy, 2015, 7, 35. | 6.2 | 129 |
| 136 | Aberrant White Matter Networks Mediate Cognitive Impairment in Patients with Silent Lacunar Infarcts in Basal Ganglia Territory. Journal of Cerebral Blood Flow and Metabolism, 2015, 35, 1426-1434. | 4.3 | 18 |
| 137 | Associations Between Biomarkers and Age in the Presenilin 1 E280A Autosomal Dominant Alzheimer Disease Kindred. JAMA Neurology, 2015, 72, 316. | 9.0 | 145 |
| 138 | Association of White Matter Integrity and Cognitive Functions in Patients With Subcortical Silent Lacunar Infarcts. Stroke, 2015, 46, 1123-1126. | 2.0 | 35 |
| 139 | Measurement of Longitudinal β-Amyloid Change with ¹⁸ F-Florbetapir PET and Standardized Uptake Value Ratios. Journal of Nuclear Medicine, 2015, 56, 567-574. | 5.0 | 273 |
| 140 | Multi-modality sparse representation-based classification for Alzheimer's disease and mild cognitive impairment. Computer Methods and Programs in Biomedicine, 2015, 122, 182-190. | 4.7 | 70 |
| 141 | Studying ventricular abnormalities in mild cognitive impairment with hyperbolic Ricci flow and tensor-based morphometry. NeuroImage, 2015, 104, 1-20. | 4.2 | 42 |
| 142 | Alzheimer Disease Biomarkers as Outcome Measures for Clinical Trials in MCI. Alzheimer Disease and Associated Disorders, 2015, 29, 101-109. | 1.3 | 14 |
| 143 | Independent Component Analysis-Based Identification of Covariance Patterns of Microstructural White Matter Damage in Alzheimer's Disease. PLoS ONE, 2015, 10, e0119714. | 2.5 | 15 |
| 144 | The Alzheimer's Prevention Initiative Composite Cognitive Test Score. Journal of Clinical Psychiatry, 2014, 75, 652-660. | 2.2 | 75 |

| # | Article | IF | CITATIONS |
|-----|--|------|-----------|
| 145 | Aging Influence on Gray Matter Structural Associations within the Default Mode Network Utilizing Bayesian Network Modeling. Frontiers in Aging Neuroscience, 2014, 6, 105. | 3.4 | 6 |
| 146 | Characterizing structural association alterations within brain networks in normal aging using Gaussian Bayesian networks. Frontiers in Computational Neuroscience, 2014, 8, 122. | 2.1 | 5 |
| 147 | A pooling-LiNGAM algorithm for effective connectivity analysis of fMRI data. Frontiers in Computational Neuroscience, 2014, 8, 125. | 2.1 | 15 |
| 148 | Biomarker Research of Preclinical Alzheimer's Disease and MCI Based on Neuroimage Techniques. Neuroscience and Biomedical Engineering, 2014, 1, 92-101. | 0.4 | 0 |
| 149 | Structural and Functional Brain Changes in the Default Mode Network in Subtypes of Amnestic Mild Cognitive Impairment. Journal of Geriatric Psychiatry and Neurology, 2014, 27, 188-198. | 2.3 | 27 |
| 150 | Neuronal injury biomarkers and prognosis in ADNI subjects with normal cognition. Acta Neuropathologica Communications, 2014, 2, 26. | 5.2 | 77 |
| 151 | Regional covariance patterns of gray matter alterations in Alzheimer's disease and its replicability evaluation. Journal of Magnetic Resonance Imaging, 2014, 39, 143-149. | 3.4 | 9 |
| 152 | Brain Differences in Infants at Differential Genetic Risk for Late-Onset Alzheimer Disease. JAMA Neurology, 2014, 71, 11. | 9.0 | 221 |
| 153 | Fibrillar amyloid correlates of preclinical cognitive decline. , 2014, 10, e1-e8. | | 15 |
| 154 | An empirically derived composite cognitive test score with improved power to track and evaluate treatments for preclinical Alzheimer's disease. Alzheimer's and Dementia, 2014, 10, 666-674. | 0.8 | 110 |
| 155 | Subjective cognitive decline: Self and informant comparisons. Alzheimer's and Dementia, 2014, 10, 93-98. | 0.8 | 111 |
| 156 | Independent component analysis of DTI data reveals white matter covariances in Alzheimer's disease. , 2014, , . | | 1 |
| 157 | P4-298: IMPROVING THE POWER TO TRACK FIBRILLAR AMYLOID PET MEASUREMENTS AND EVALUATE AMYLOID-MODIFYING TREATMENTS USING A CEREBRAL WHITE MATTER REFERENCE REGION-OF-INTEREST. , 2014, 10, P894-P894. | | 0 |
| 158 | A Statistical Parametric Mapping Toolbox Used for Voxel-Wise Analysis of FDG-PET Images of Rat Brain. PLoS ONE, 2014, 9, e108295. | 2.5 | 51 |
| 159 | A rat brain MRI template with digital stereotaxic atlas of fine anatomical delineations in paxinos space and its automated application in voxelâ€wise analysis. Human Brain Mapping, 2013, 34, 1306-1318. | 3.6 | 105 |
| 160 | Ushering in the study and treatment of preclinical Alzheimer disease. Nature Reviews Neurology, 2013, 9, 371-381. | 10.1 | 125 |
| 161 | Genetic Susceptibility for Alzheimer Disease Neuritic Plaque Pathology. JAMA Neurology, 2013, 70, 1150. | 9.0 | 143 |
| 162 | Fast direct estimation of the blood input function and myocardial time activity curve from dynamic SPECT projections via reduction in spatial and temporal dimensions. Medical Physics, 2013, 40, 092503. | 3.0 | 14 |

| # | Article | IF | CITATIONS |
|-----|--|------|-----------|
| 163 | Clinical and multimodal biomarker correlates of ADNI neuropathological findings. Acta Neuropathologica Communications, 2013, 1, 65. | 5.2 | 138 |
| 164 | Overfeeding Over 24 Hours Does Not Activate Brown Adipose Tissue in Humans. Journal of Clinical Endocrinology and Metabolism, 2013, 98, E1956-E1960. | 3.6 | 39 |
| 165 | The Receiver Operational Characteristic for Binary Classification with Multiple Indices and Its Application to the Neuroimaging Study of Alzheimer's Disease. IEEE/ACM Transactions on Computational Biology and Bioinformatics, 2013, 10, 173-180. | 3.0 | 20 |
| 166 | Combining Multiple Markers to Improve the Longitudinal Rate of Progression: Application to Clinical Trials on the Early Stage of Alzheimer's Disease. Statistics in Biopharmaceutical Research, 2013, 5, 54-66. | 0.8 | 11 |
| 167 | Apolipoprotein E Îμ4 and age effects on florbetapir positron emission tomography in healthy aging and Alzheimer disease. Neurobiology of Aging, 2013, 34, 1-12. | 3.1 | 208 |
| 168 | A Sparse Structure Learning Algorithm for Gaussian Bayesian Network Identification from High-Dimensional Data. IEEE Transactions on Pattern Analysis and Machine Intelligence, 2013, 35, 1328-1342. | 13.9 | 54 |
| 169 | Polymorphism of brain derived neurotrophic factor influences β amyloid load in cognitively intact apolipoprotein E ε4 carriers. Neurolmage: Clinical, 2013, 2, 512-520. | 2.7 | 47 |
| 170 | Antidepressant effects of sertraline associated with volume increases in dorsolateral prefrontal cortex. Journal of Affective Disorders, 2013, 146, 414-419. | 4.1 | 80 |
| 171 | O2-03-01: Validation of the Alzheimer's Prevention Initiative Composite Cognitive Test Score. , 2013, 9, P320-P320. | | 0 |
| 172 | Higher serum glucose levels are associated with cerebral hypometabolism in Alzheimer regions. Neurology, 2013, 80, 1557-1564. | 1.1 | 83 |
| 173 | O4-08-01: Association between the Alzheimer's disease-related hypometabolic convergence index and clinical ratings in cognitively normal older adults with and without significant fibrillar amyloid burden: Findings from the Alzheimer's Disease Neuroimaging. , 2013, 9, P698-P698. | | 0 |
| 174 | Alzheimer's disease-related changes in regional spontaneous brain activity levels and inter-region interactions in the default mode network. Brain Research, 2013, 1509, 58-65. | 2.2 | 14 |
| 175 | Diagnostic accuracy of markers for prodromal Alzheimer's disease in independent clinical series. Alzheimer's and Dementia, 2013, 9, 677-686. | 0.8 | 51 |
| 176 | Improved Estimation of the Number of Independent Components for Functional Magnetic Resonance Data by a Whitening Filter. IEEE Journal of Biomedical and Health Informatics, 2013, 17, 629-641. | 6.3 | 11 |
| 177 | Pro-inflammatory cytokine network in peripheral inflammation response to cerebral ischemia. Neuroscience Letters, 2013, 548, 4-9. | 2.1 | 41 |
| 178 | Separating 4D multi-task fMRI data of multiple subjects by independent component analysis with projection. Magnetic Resonance Imaging, 2013, 31, 60-74. | 1.8 | 2 |
| 179 | Fat-free body mass but not fat mass is associated with reduced gray matter volume of cortical brain regions implicated in autonomic and homeostatic regulation. NeuroImage, 2013, 64, 712-721. | 4.2 | 45 |
| 180 | Prevalence of and Potential Risk Factors for Mild Cognitive Impairment in Communityâ€Dwelling Residents of Beijing. Journal of the American Geriatrics Society, 2013, 61, 2111-2119. | 2.6 | 75 |

| # | Article | IF | CITATIONS |
|-----|---|------|-----------|
| 181 | Alterations of Directional Connectivity among Resting-State Networks in Alzheimer Disease. American Journal of Neuroradiology, 2013, 34, 340-345. | 2.4 | 39 |
| 182 | Posterior Cingulate Glucose Metabolism, Hippocampal Glucose Metabolism, and Hippocampal Volume in Cognitively Normal, Late-Middle-Aged Persons at 3 Levels of Genetic Risk for Alzheimer Disease. JAMA Neurology, 2013, 70, 320. | 9.0 | 123 |
| 183 | A Semi-Automated Region of Interest Detection Method in the Scintigraphic Glomerular Filtration Rate Determination for Patients With Abnormal Low Renal Function. Clinical Nuclear Medicine, 2013, 38, 855-862. | 1.3 | 11 |
| 184 | Effects of Memantine on Clinical Ratings, Fluorodeoxyglucose Positron Emission Tomography Measurements, and Cerebrospinal Fluid Assays in Patients With Moderate to Severe Alzheimer Dementia. Journal of Clinical Psychopharmacology, 2013, 33, 636-642. | 1.4 | 29 |
| 185 | Different Patterns of White Matter Disruption among Amnestic Mild Cognitive Impairment Subtypes: Relationship with Neuropsychological Performance. Journal of Alzheimer's Disease, 2013, 36, 365-376. | 2.6 | 32 |
| 186 | Separating lexical-semantic access from other mnemonic processes in picture-name verification. Frontiers in Psychology, 2013, 4, 706. | 2.1 | 6 |
| 187 | Identifying effective connectivity parameters in simulated fMRI: a direct comparison of switching linear dynamic system, stochastic dynamic causal, and multivariate autoregressive models. Frontiers in Neuroscience, 2013, 7, 70. | 2.8 | 7 |
| 188 | Association between an Alzheimer's Disease-Related Index and APOE ε4 Gene Dose. PLoS ONE, 2013, 8, e67163. | 2.5 | 13 |
| 189 | Regional Neural Response Differences in the Determination of Faces or Houses Positioned in a Wide Visual Field. PLoS ONE, 2013, 8, e72728. | 2.5 | 9 |
| 190 | Structural Interactions within the Default Mode Network Identified by Bayesian Network Analysis in Alzheimer's Disease. PLoS ONE, 2013, 8, e74070. | 2.5 | 16 |
| 191 | Whole Brain Atrophy and Sample Size Estimate via Iterative Principal Component Analysis for Twelve-month Alzheimer's Disease Trials. Neuroscience and Biomedical Engineering, 2013, 1, 40-47. | 0.4 | 6 |
| 192 | Summary Metrics to Assess Alzheimer Disease–Related Hypometabolic Pattern with ¹⁸ F-FDG PET: Head-to-Head Comparison. Journal of Nuclear Medicine, 2012, 53, 592-600. | 5.0 | 79 |
| 193 | Primary motor cortex activity reduction under the regulation of SMA by real-time fMRI. , 2012, , . | | 0 |
| 194 | A method for generating image-derived input function in quantitative 18F-FDG PET study based on the monotonicity of the input and output function curve. Nuclear Medicine Communications, 2012, 33, 362-370. | 1.1 | 14 |
| 195 | Cerebral blood flow in Alzheimer's disease. Vascular Health and Risk Management, 2012, 8, 599. | 2.3 | 162 |
| 196 | Brain imaging and fluid biomarker analysis in young adults at genetic risk for autosomal dominant Alzheimer's disease in the presenilin 1 E280A kindred: a case-control study. Lancet Neurology, The, 2012, 11, 1048-1056. | 10.2 | 450 |
| 197 | Mapping joint grey and white matter reductions in Alzheimer's disease using joint independent component analysis. Neuroscience Letters, 2012, 531, 136-141. | 2.1 | 26 |
| | | _ | - |

198 Structural correlation in the default mode network in Alzheimer's disease. , 2012, , .

0

KEWEI CHEN

| # | Article | IF | CITATIONS |
|-----|--|------|-----------|
| 199 | A transfer learning approach for network modeling. IIE Transactions, 2012, 44, 915-931. | 2.1 | 19 |
| 200 | Blood pressure is associated with higher brain amyloid burden and lower glucose metabolism in healthy late middle-age persons. Neurobiology of Aging, 2012, 33, 827.e11-827.e19. | 3.1 | 109 |
| 201 | Gray matter network associated with risk for Alzheimer's disease in young to middle-aged adults. Neurobiology of Aging, 2012, 33, 2723-2732. | 3.1 | 81 |
| 202 | Temporal and instantaneous connectivity of default mode network estimated using Gaussian Bayesian network frameworks. Neuroscience Letters, 2012, 513, 62-66. | 2.1 | 5 |
| 203 | Lysosomal targeting of phafin1 mediated by Rab7 induces autophagosome formation. Biochemical and Biophysical Research Communications, 2012, 417, 35-42. | 2.1 | 22 |
| 204 | Florbetapir PET analysis of amyloid-β deposition in the presenilin 1 E280A autosomal dominant Alzheimer's disease kindred: a cross-sectional study. Lancet Neurology, The, 2012, 11, 1057-1065. | 10.2 | 209 |
| 205 | Postprandial plasma PYY concentrations are associated with increased regional gray matter volume and rCBF declines in caudate nuclei — A combined MRI and H215O PET study. NeuroImage, 2012, 60, 592-600. | 4.2 | 13 |
| 206 | Correlations between FDG PET glucose uptake-MRI gray matter volume scores and apolipoprotein E ε4 gene dose in cognitively normal adults: A cross-validation study using voxel-based multi-modal partial least squares. NeuroImage, 2012, 60, 2316-2322. | 4.2 | 36 |
| 207 | Attentionâ€related networks in Alzheimer's disease: A resting functional MRI study. Human Brain Mapping, 2012, 33, 1076-1088. | 3.6 | 110 |
| 208 | Wavelet-Based De-noising of Positron Emission Tomography Scans. Journal of Scientific Computing, 2012, 50, 665-677. | 2.3 | 12 |
| 209 | An fMRI Study of the Neural Systems Involved in Visually Cued Auditory Top-Down Spatial and Temporal Attention. PLoS ONE, 2012, 7, e49948. | 2.5 | 33 |
| 210 | Accurate measurement of brain changes in longitudinal MRI scans using tensor-based morphometry. NeuroImage, 2011, 57, 5-14. | 4.2 | 77 |
| 211 | Large-scale directional connections among multi resting-state neural networks in human brain: A functional MRI and Bayesian network modeling study. NeuroImage, 2011, 56, 1035-1042. | 4.2 | 49 |
| 212 | Association between GAB2 haplotype and higher glucose metabolism in Alzheimer's disease-affected brain regions in cognitively normal APOEÎμ4 carriers. NeuroImage, 2011, 54, 1896-1902. | 4.2 | 22 |
| 213 | Using Positron Emission Tomography and Florbetapir F 18 to Image Cortical Amyloid in Patients With Mild Cognitive Impairment or Dementia Due to Alzheimer Disease. Archives of Neurology, 2011, 68, 1404. | 4.5 | 310 |
| 214 | Neural substrates in color processing: A comparison between painting majors and non-majors. Neuroscience Letters, 2011, 487, 191-195. | 2.1 | 9 |
| 215 | Characterizing Alzheimer's disease using a hypometabolic convergence index. NeuroImage, 2011, 56, 52-60. | 4.2 | 144 |
| 216 | A Multi-Center Randomized Proof-of-Concept Clinical Trial Applying [18F]FDG-PET for Evaluation of Metabolic Therapy with Rosiglitazone XR in Mild to Moderate Alzheimer's Disease. Journal of Alzheimer's Disease, 2011, 22, 1241-1256. | 2.6 | 86 |

| # | Article | IF | CITATIONS |
|-----|--|-----|-----------|
| 217 | A method of generating image-derived input function in a quantitative 18F-FDG PET study based on the shape of the input function curve. Nuclear Medicine Communications, 2011, 32, 1121-1127. | 1.1 | 10 |
| 218 | Machine Learning Approaches for the Neuroimaging Study of Alzheimer's Disease. Computer, 2011, 44, 99-101. | 1.1 | 40 |
| 219 | Altered default mode network connectivity in alzheimer's disease—A resting functional MRI and bayesian network study. Human Brain Mapping, 2011, 32, 1868-1881. | 3.6 | 172 |
| 220 | Positron Emission Tomography and Neuropathologic Estimates of Fibrillar Amyloid-β in a Patient With Down Syndrome and Alzheimer Disease. Archives of Neurology, 2011, 68, 1461. | 4.5 | 51 |
| 221 | Brain effective connectivity modeling for alzheimer's disease by sparse gaussian bayesian network. , 2011, , 931-939. | | 24 |
| 222 | A resting-state functional MRI study of the post-effect of acupuncture. , 2011, , . | | 0 |
| 223 | Altered Connectivity Pattern of Hubs in Default-Mode Network with Alzheimer's Disease: An Granger Causality Modeling Approach. PLoS ONE, 2011, 6, e25546. | 2.5 | 71 |
| 224 | The application of independent component analysis with projection method to two-task fMRI data over multiple subjects. , 2011, , . | | 2 |
| 225 | Comparison of gray matter volume and thickness for analysis of cortical changes in Alzheimer's disease. Proceedings of SPIE, 2011, , . | 0.8 | 2 |
| 226 | The simulation of land use type change in Erhai Basin based on agent based modeling. , 2011, , . | | 2 |
| 227 | Image-Derived Input Function for Brain PET Studies: Many Challenges and Few Opportunities. Journal of Cerebral Blood Flow and Metabolism, 2011, 31, 1986-1998. | 4.3 | 246 |
| 228 | Alzheimer's Prevention Initiative: A Plan to Accelerate the Evaluation of Presymptomatic Treatments. Journal of Alzheimer's Disease, 2011, 26, 321-329. | 2.6 | 309 |
| 229 | Effective Connectivity Modeling for fMRI: Six Issues and Possible Solutions Using Linear Dynamic Systems. Frontiers in Systems Neuroscience, 2011, 5, 104. | 2.5 | 23 |
| 230 | Mapping gray matter volume and cortical thickness in Alzheimer's disease. , 2010, , . | | 1 |
| 231 | The improvement of ICA with projection technique in multitask fMRI data analysis. Proceedings of SPIE, 2010, , . | 0.8 | 0 |
| 232 | Assessing the reliability to detect cerebral hypometabolism in probable Alzheimer's disease and amnestic mild cognitive impairment. Journal of Neuroscience Methods, 2010, 192, 277-285. | 2.5 | 14 |
| 233 | Association of CR1, CLU and PICALM with Alzheimer's disease in a cohort of clinically characterized and neuropathologically verified individuals. Human Molecular Genetics, 2010, 19, 3295-3301. | 2.9 | 223 |
| 234 | Hypometabolism in Alzheimer-Affected Brain Regions in Cognitively Healthy Latino Individuals Carrying the Apolipoprotein E ε4 Allele. Archives of Neurology, 2010, 67, 462-8. | 4.5 | 89 |

KEWEI CHEN

| # | Article | IF | CITATIONS |
|-----|--|-----|-----------|
| 235 | Twelve-month metabolic declines in probable Alzheimer's disease and amnestic mild cognitive impairment assessed using an empirically pre-defined statistical region-of-interest: Findings from the Alzheimer's Disease Neuroimaging Initiative. NeuroImage, 2010, 51, 654-664. | 4.2 | 145 |
| 236 | Deriving difference between the Bayesian networks based patterns of the effective connectivity using permutation test in fMRI studies. , 2010, , . | | 1 |
| 237 | Voxel-based assessment of gray and white matter volumes in Alzheimer's disease. Neuroscience Letters, 2010, 468, 146-150. | 2.1 | 128 |
| 238 | Reducing modeling error of graphical methods for estimating volume of distribution measurements in PIB–PET study. Mathematical Biosciences, 2010, 226, 134-146. | 1.9 | 4 |
| 239 | Evidence for an association between KIBRA and late-onset Alzheimer's disease. Neurobiology of Aging, 2010, 31, 901-909. | 3.1 | 100 |
| 240 | Whole brain atrophy rate predicts progression from MCI to Alzheimer's disease. Neurobiology of Aging, 2010, 31, 1601-1605. | 3.1 | 45 |
| 241 | The Alzheimer's Disease Neuroimaging Initiative positron emission tomography core. Alzheimer's and Dementia, 2010, 6, 221-229. | 0.8 | 464 |
| 242 | Higher serum total cholesterol levels in late middle age are associated with glucose hypometabolism in brain regions affected by Alzheimer's disease and normal aging. NeuroImage, 2010, 49, 169-176. | 4.2 | 61 |
| 243 | Age-related networks of regional covariance in MRI gray matter: Reproducible multivariate patterns in healthy aging. NeuroImage, 2010, 49, 1750-1759. | 4.2 | 113 |
| 244 | Imaging systems level consolidation of novel associate memories: A longitudinal neuroimaging study. NeuroImage, 2010, 50, 826-836. | 4.2 | 17 |
| 245 | Identification and validation of effective connectivity networks in functional magnetic resonance imaging using switching linear dynamic systems. NeuroImage, 2010, 52, 1027-1040. | 4.2 | 43 |
| 246 | Learning brain connectivity of Alzheimer's disease by sparse inverse covariance estimation. NeuroImage, 2010, 50, 935-949. | 4.2 | 280 |
| 247 | Application of Granger causality analysis to effective connectivity of the default-mode network. , 2010, , . | | 1 |
| 248 | Applications of Neuroimaging to Disease-Modification Trials in Alzheimer's Disease. Behavioural Neurology, 2009, 21, 129-136. | 2.1 | 17 |
| 249 | Fibrillar amyloid-β burden in cognitively normal people at 3 levels of genetic risk for Alzheimer's disease. Proceedings of the National Academy of Sciences of the United States of America, 2009, 106, 6820-6825. | 7.1 | 700 |
| 250 | Functional network connectivity analysis based on partial correlation in Alzheimer's disease. , 2009, , . | | 0 |
| 251 | Mapping brain development during childhood, adolescence and young adulthood. Proceedings of SPIE, 2009, , . | 0.8 | 0 |
| 252 | Mining brain region connectivity for alzheimer's disease study via sparse inverse covariance | | 37 |

estimation., 2009,,.

| # | Article | IF | CITATIONS |
|-----|---|-----|-----------|
| 253 | Effective connectivity analysis of default mode network based on the Bayesian network learning approach. Proceedings of SPIE, 2009, , . | 0.8 | 5 |
| 254 | An improved exponential filter for fast nonlinear registration of brain magnetic resonance images. Progress in Natural Science: Materials International, 2009, 19, 759-767. | 4.4 | 1 |
| 255 | Improved application of independent component analysis to functional magnetic resonance imaging study via linear projection techniques. Human Brain Mapping, 2009, 30, 417-431. | 3.6 | 14 |
| 256 | Improved interâ€modality image registration using normalized mutual information with coarseâ€binned histograms. Communications in Numerical Methods in Engineering, 2009, 25, 583-595. | 1.3 | 7 |
| 257 | FDG–PET parametric imaging by total variation minimization. Computerized Medical Imaging and Graphics, 2009, 33, 295-303. | 5.8 | 17 |
| 258 | The value of positron emission tomography and proliferation index in predicting progression in low-grade astrocytomas of childhood. Journal of Neuro-Oncology, 2009, 95, 239-245. | 2.9 | 38 |
| 259 | Reanalysis of the Obesity-Related Attenuation in the Left Dorsolateral Prefrontal Cortex Response to a Satiating Meal Using Gyral Regions-of-Interest. Journal of the American College of Nutrition, 2009, 28, 667-673. | 1.8 | 31 |
| 260 | Sparse Inverse Covariance Analysis of human brain for Alzheimer's disease study. , 2009, , . | | 2 |
| 261 | Whole brain atrophy based on iterative principal component analysis and MRI techniques in the study of Alzheimer's disease. , 2009, , . | | 2 |
| 262 | Using the Artificial Neural Network to discriminate between normal controls with different APOE e4 genotypes and probable AD cases in PIB-PET studies. , 2009, , . | | 1 |
| 263 | Reducing the noise effects in Logan graphic analysis for PET receptor measurements. , 2009, , . | | 1 |
| 264 | Automation of the Logan plot based PiB-PET quantification over multiple subjects and multiple reference regions. , 2009, , . | | 0 |
| 265 | Neural correlates of heart rate variability during emotion. NeuroImage, 2009, 44, 213-222. | 4.2 | 588 |
| 266 | Multiple neural networks supporting a semantic task: An fMRI study using independent component analysis. NeuroImage, 2009, 45, 1347-1358. | 4.2 | 38 |
| 267 | Categorical and correlational analyses of baseline fluorodeoxyglucose positron emission tomography images from the Alzheimer's Disease Neuroimaging Initiative (ADNI). NeuroImage, 2009, 45, 1107-1116. | 4.2 | 258 |
| 268 | Linking functional and structural brain images with multivariate network analyses: A novel application of the partial least square method. NeuroImage, 2009, 47, 602-610. | 4.2 | 65 |
| 269 | Resting-state BOLD networks versus task-associated functional MRI for distinguishing Alzheimer's disease risk groups. Neurolmage, 2009, 47, 1678-1690. | 4.2 | 201 |
| 270 | Applications of neuroimaging to disease-modification trials in Alzheimer's disease. Behavioural Neurology, 2009, 21, 129-36. | 2.1 | 14 |

| # | Article | IF | CITATIONS |
|-----|--|-----|-----------|
| 271 | Interpreting scan data acquired from multiple scanners: A study with Alzheimer's disease. NeuroImage, 2008, 39, 1180-1185. | 4.2 | 200 |
| 272 | Cholesterol-related genetic risk scores are associated with hypometabolism in Alzheimer's-affected brain regions. Neurolmage, 2008, 40, 1214-1221. | 4.2 | 30 |
| 273 | Association between trait emotional awareness and dorsal anterior cingulate activity during emotion is arousal-dependent. Neurolmage, 2008, 41, 648-655. | 4.2 | 151 |
| 274 | Age-Related Regional Network of Magnetic Resonance Imaging Gray Matter in the Rhesus Macaque. Journal of Neuroscience, 2008, 28, 2710-2718. | 3.6 | 78 |
| 275 | Heterogeneous data fusion for alzheimer's disease study. , 2008, , . | | 75 |
| 276 | Correlating Cerebral Hypometabolism With Future Memory Decline in Subsequent Converters to Amnestic Pre–Mild Cognitive Impairment. Archives of Neurology, 2008, 65, 1231-6. | 4.5 | 91 |
| 277 | Ipsilateral brain deactivation specific to the nondominant hand during simple finger movements. NeuroReport, 2008, 19, 483-486. | 1.2 | 13 |
| 278 | Correlations Between Apolipoprotein E ε4 Gene Dose and Whole Brain Atrophy Rates. American Journal of Psychiatry, 2007, 164, 916-921. | 7.2 | 104 |
| 279 | Characterization of the image-derived carotid artery input function using independent component analysis for the quantitation of [18F] fluorodeoxyglucose positron emission tomography images. Physics in Medicine and Biology, 2007, 52, 7055-7071. | 3.0 | 107 |
| 280 | A Monte-Carlo Simulation Package, Multiple Comparison Corrections and Power Estimation Incorporating Secondary Supportive Evidence. , 2007, , . | | 0 |
| 281 | Automated diagnosis and prediction of Alzheimer disease using magnetic resonance image. , 2007, , . | | 0 |
| 282 | Brain development in Chinese children and adolescents: a structural MRI study. NeuroReport, 2007, 18, 875-880. | 1.2 | 33 |
| 283 | An input function estimation method for FDG-PET human brain studies. Nuclear Medicine and Biology, 2007, 34, 483-492. | 0.6 | 38 |
| 284 | Relationships between plasma leptin concentrations and human brain structure: A voxel-based morphometric study. Neuroscience Letters, 2007, 412, 248-253. | 2.1 | 72 |
| 285 | Postprandial glucagon-like peptide-1 (GLP-1) response is positively associated with changes in neuronal activity of brain areas implicated in satiety and food intake regulation in humans. NeuroImage, 2007, 35, 511-517. | 4.2 | 112 |
| 286 | Inter-Frame Co-Registration of Dynamically Acquired Fluoro-Deoxyglucose Positron Emission Tomography Human Brain Data. , 2007, , . | | 3 |
| 287 | Less activation in the left dorsolateral prefrontal cortex in the reanalysis of the response to a meal in obese than in lean women and its association with successful weight loss. American Journal of Clinical Nutrition, 2007, 86, 573-579. | 4.7 | 113 |
| 288 | A variant of logistic transfer function in Infomax and a postprocessing procedure for independent component analysis applied to fMRI data. Magnetic Resonance Imaging, 2007, 25, 703-711. | 1.8 | 4 |

| # | Article | IF | CITATIONS |
|-----|--|-----|-----------|
| 289 | Is the brain representation of hunger normal in the Prader-Willi syndrome?. International Journal of Obesity, 2007, 31, 390-390. | 3.4 | 1 |
| 290 | Successful dieters have increased neural activity in cortical areas involved in the control of behavior. International Journal of Obesity, 2007, 31, 440-448. | 3.4 | 204 |
| 291 | Correlations Between Apolipoprotein E ε4 Gene Dose and Whole Brain Atrophy Rates. American Journal of Psychiatry, 2007, 164, 916. | 7.2 | 29 |
| 292 | Network analysis of single-subject fMRI during a finger opposition task. NeuroImage, 2006, 32, 325-332. | 4.2 | 35 |
| 293 | Brain abnormalities in human obesity: A voxel-based morphometric study. NeuroImage, 2006, 31, 1419-1425. | 4.2 | 459 |
| 294 | Activation of brain regions vulnerable to Alzheimer's disease: The effect of mild cognitive impairment. Neurobiology of Aging, 2006, 27, 1604-1612. | 3.1 | 228 |
| 295 | A Preliminary Fluorodeoxyglucose Positron Emission Tomography Study in Healthy Adults Reporting Dream-Enactment Behavior. Sleep, 2006, 29, 927-933. | 1.1 | 51 |
| 296 | Less activation of the left dorsolateral prefrontal cortex in response to a meal: a feature of obesity. American Journal of Clinical Nutrition, 2006, 84, 725-731. | 4.7 | 151 |
| 297 | A new post-processing method of applying independent component analysis to fMRI data. , 2006, , . | | 1 |
| 298 | Regional network of magnetic resonance imaging gray matter volume in healthy aging. NeuroReport, 2006, 17, 951-956. | 1.2 | 74 |
| 299 | Regional gray matter abnormalities in patients with schizophrenia determined with optimized voxel-based morphometry. , 2006, , . | | 1 |
| 300 | An automated normative-based fluorodeoxyglucose positron emission tomography image-analysis procedure to aid Alzheimer disease diagnosis using statistical parametric mapping and interactive image display. , 2006, 6144, 1638. | | 1 |
| 301 | Arithmetic processing in the brain shaped by cultures. Proceedings of the National Academy of Sciences of the United States of America, 2006, 103, 10775-10780. | 7.1 | 306 |
| 302 | Constructing and assessing brain templates from Chinese pediatric MRI data using SPM. , 2005, , . | | 0 |
| 303 | Cerebral asymmetry in children when reading Chinese characters. Cognitive Brain Research, 2005, 24, 206-214. | 3.0 | 39 |
| 304 | Correlations between apolipoprotein E ε4 gene dose and brain-imaging measurements of regional hypometabolism. Proceedings of the National Academy of Sciences of the United States of America, 2005, 102, 8299-8302. | 7.1 | 366 |
| 305 | Sensory experience of food and obesity: a positron emission tomography study of the brain regions affected by tasting a liquid meal after a prolonged fast. NeuroImage, 2005, 24, 436-443. | 4.2 | 139 |
| | | | |

MRI Template and Atlas Toolbox for the C57BL/6J Mouse Brain. , 2005, , .

| # | Article | IF | CITATIONS |
|-----|---|-----|-----------|
| 307 | Functional brain abnormalities in young adults at genetic risk for late-onset Alzheimer's dementia. Proceedings of the National Academy of Sciences of the United States of America, 2004, 101, 284-289. | 7.1 | 907 |
| 308 | Persistence of abnormal neural responses to a meal in postobese individuals. International Journal of Obesity, 2004, 28, 370-377. | 3.4 | 159 |
| 309 | Positron Emission Tomography and Magnetic Resonance Imaging in the Study of Cognitively Normal Persons at Differential Genetic Risk for Alzheimer's Dementia. , 2004, , 151-177. | | 2 |
| 310 | An automated algorithm for the computation of brain volume change from sequential MRIs using an iterative principal component analysis and its evaluation for the assessment of whole-brain atrophy rates in patients with probable Alzheimer's disease. NeuroImage, 2004, 22, 134-143. | 4.2 | 48 |
| 311 | Are We Addicted to Food?. Obesity, 2003, 11, 493-495. | 4.0 | 52 |
| 312 | Clustering huge data sets for parametric PET imaging. BioSystems, 2003, 71, 81-92. | 2.0 | 64 |
| 313 | Improving tissue segmentation of human brain MRI through preprocessing by the Gegenbauer reconstruction method. NeuroImage, 2003, 20, 489-502. | 4.2 | 38 |
| 314 | Monte-Carlo based neuroimaging set-level multiple-comparison correction. IFAC Postprint Volumes IPPV / International Federation of Automatic Control, 2003, 36, 11-15. | 0.4 | 4 |
| 315 | Construction of mouse brain MRI templates using SPM 99. IFAC Postprint Volumes IPPV / International Federation of Automatic Control, 2003, 36, 113-118. | 0.4 | 1 |
| 316 | Longitudinal PET Evaluation of Cerebral Metabolic Decline in Dementia: A Potential Outcome Measure in Alzheimer's Disease Treatment Studies. American Journal of Psychiatry, 2002, 159, 738-745. | 7.2 | 437 |
| 317 | Tasting a liquid meal after a prolonged fast is associated with preferential activation of the left hemisphere. NeuroReport, 2002, 13, 1141-1145. | 1.2 | 39 |
| 318 | Sex differences in the human brain's response to hunger and satiation. American Journal of Clinical Nutrition, 2002, 75, 1017-1022. | 4.7 | 120 |
| 319 | Effects of Image Resolution on Autoradiographic Measurements of Posterior Cingulate Activity in PDAPP Mice: Implications for Functional Brain Imaging Studies of Transgenic Mouse Models of Alzheimer's Disease. NeuroImage, 2002, 16, 1-6. | 4.2 | 33 |
| 320 | Neuroimaging and Obesity. Annals of the New York Academy of Sciences, 2002, 967, 389-397. | 3.8 | 159 |
| 321 | Neuroimaging and obesity: mapping the brain responses to hunger and satiation in humans using positron emission tomography. Annals of the New York Academy of Sciences, 2002, 967, 389-97. | 3.8 | 87 |
| 322 | Effect of Satiation on Brain Activity in Obese and Lean Women. Obesity, 2001, 9, 676-684. | 4.0 | 184 |
| 323 | Tracking the decline in cerebral glucose metabolism in persons and laboratory animals at genetic risk for Alzheimer's disease. Clinical Neuroscience Research, 2001, 1, 194-206. | 0.8 | 26 |
| 324 | Declining brain activity in cognitively normal apolipoprotein E É>4 heterozygotes: A foundation for using positron emission tomography to efficiently test treatments to prevent Alzheimer's disease. Proceedings of the National Academy of Sciences of the United States of America, 2001, 98, 3334-3339. | 7.1 | 444 |

| # | Article | IF | CITATIONS |
|-----|--|------|-----------|
| 325 | Functional brain mapping using positron emission tomography scanning in preoperative neurosurgical planning for pediatric brain tumors. Neurosurgical Focus, 2000, 8, 1-7. | 2.3 | 0 |
| 326 | Tracking Alzheimer's disease in transgenic mice using fluorodeoxyglucose autoradiography. NeuroReport, 2000, 11, 987-991. | 1.2 | 63 |
| 327 | Regional myocardial oxygen consumption estimated by carbon-11 acetate and positron emission tomography before and after repetitive ischemiaa 	†a 	†a 	ta 	ta 	ta 	ta 	ta 	ta 	ta 	ta 	ta 	t | 2.1 | 4 |
| 328 | Thermosensory activation of insular cortex. Nature Neuroscience, 2000, 3, 184-190. | 14.8 | 883 |
| 329 | Three Cases of Primary Hyperparathyroidism (PHP) with Prior Failed Surgery Where Culprit Lesions Were Identified by 11C-Methionine Positron Emission Tomography (PET) and Accurately Localized with PET-MRI Coregistration. Molecular Imaging and Biology, 2000, 3, 31-36. | 0.3 | 5 |
| 330 | Regions of the human brain affected during a liquid-meal taste perception in the fasting state: a positron emission tomography study. American Journal of Clinical Nutrition, 1999, 70, 806-810. | 4.7 | 67 |
| 331 | Functional brain mapping using positron emission tomography scanning in preoperative neurosurgical planning for pediatric brain tumors. Journal of Neurosurgery, 1999, 91, 797-803. | 1.6 | 70 |
| 332 | Neuroanatomical correlates of hunger and satiation in humans using positron emission tomography. Proceedings of the National Academy of Sciences of the United States of America, 1999, 96, 4569-4574. | 7.1 | 549 |
| 333 | Visceral adipose tissue is not increased in Pima Indians compared with equally obese Caucasians and is not related to insulin action or secretion. Diabetologia, 1999, 42, 28-34. | 6.3 | 48 |
| 334 | Medial temporal lobe activation during episodic encoding and retrieval: A PET study. , 1999, 9, 575-581. | | 55 |
| 335 | Noninvasive Quantification of the Cerebral Metabolic Rate for Glucose Using Positron Emission Tomography, 18F-Fluoro-2-Deoxyglucose, the Patlak Method, and an Image-Derived Input Function. Journal of Cerebral Blood Flow and Metabolism, 1998, 18, 716-723. | 4.3 | 286 |
| 336 | New method for the analysis of multiple positron emission tomography dynamic datasets: an example applied to the estimation of the cerebral metabolic rate of oxygen. Medical and Biological Engineering and Computing, 1998, 36, 83-90. | 2.8 | 2 |
| 337 | Generalized linear least squares method for fast generation of myocardial blood flow parametric images with N-13 ammonia PET. IEEE Transactions on Medical Imaging, 1998, 17, 236-243. | 8.9 | 48 |
| 338 | Effects of size and orientation change on hippocampal activation during episodic recognition. NeuroReport, 1997, 8, 3993-3998. | 1.2 | 41 |
| 339 | Use of Positron Emission Tomography for Presurgical Localization of Eloquent Brain Areas in Children with Seizures. Pediatric Neurosurgery, 1997, 26, 144-156. | 0.7 | 61 |
| 340 | Positron Emission Tomography in Children With Neurofibromatosis-1. Journal of Child Neurology, 1997, 12, 499-506. | 1.4 | 37 |
| 341 | Dynamic image data compression in spatial and temporal domains: theory and algorithm. IEEE Transactions on Information Technology in Biomedicine, 1997, 1, 219-228. | 3.2 | 28 |
| 342 | Preclinical Evidence of Alzheimer's Disease in Persons Homozygous for the ε4 Allele for Apolipoprotein E. New England Journal of Medicine, 1996, 334, 752-758. | 27.0 | 1,320 |

| # | Article | IF | CITATIONS |
|-----|---|-----|-----------|
| 343 | Optimal image sampling schedule: a new effective way to reduce dynamic image storage space and functional image processing time. IEEE Transactions on Medical Imaging, 1996, 15, 710-719. | 8.9 | 54 |
| 344 | <title>Generalized linear least squares method for estimating myocardial blood flow with N-13 ammonia positron emission tomography</title> . , 1996, , . | | 0 |
| 345 | Methods for the correction of vascular artifacts in PET O-15 water brain-mapping studies. IEEE Transactions on Nuclear Science, 1996, 43, 3308-3314. | 2.0 | 4 |
| 346 | Decay correction methods in dynamic PET studies. IEEE Transactions on Nuclear Science, 1995, 42, 2173-2179. | 2.0 | 7 |
| 347 | An evaluation of the algorithms for determining local cerebral metabolic rates of glucose using positron emission tomography dynamic data. IEEE Transactions on Medical Imaging, 1995, 14, 697-710. | 8.9 | 77 |
| 348 | New estimation methods that directly use the time accumulated counts in the input function in quantitative dynamic PET studies. Physics in Medicine and Biology, 1994, 39, 2073-2090. | 3.0 | 10 |
| 349 | Simultaneous analysis of noisy signals obtained from multiple experiments, with application to deriving brain functional images. , 0, , . | | 0 |
| 350 | Adaptive smoothing strategies to eliminate the scalp/ventricle artifact in statistical parametric mapping. , 0, , . | | 0 |